



A Novel 3-Dimensional Co-culture Method Reveals a Partial Mesenchymal to Epithelial Transition in Breast Cancer Cells Induced by Adipocytes

Nikitha K. Pallegar¹ · Chantae J. Garland¹ · Mathepan Mahendralingam² · Alicia M. Vilorio-Petit² · Sherri L. Christian¹

Received: 28 June 2018 / Accepted: 2 November 2018 / Published online: 24 November 2018
© Springer Science+Business Media, LLC, part of Springer Nature 2018

Abstract

Cancer metastases are accountable for almost 90% of all human cancer related deaths including from breast cancer (BC). Adipocytes can alter the tumor microenvironment, which can promote metastasis by inducing an epithelial-to-mesenchymal transition (EMT) in BC cells. However, the role of adipocytes during the mesenchymal-to-epithelial transition (MET), that can be important in metastasis, is not clear. To understand the effect of adipocytes on the BC progression, there is a requirement for a better in vitro 3-dimensional (3D) co-culture system that mimics the breast tissue and allows for more accurate analysis of EMT and MET. We developed a co-culture system to analyze the relationship of BC cells grown in a 3D culture with adipocytes. We found that adipocytes and adipocyte-derived conditioned media, but not pre-adipocytes, caused the mesenchymal MDA-MB-231 and Hs578t cells to form significantly more epithelial-like structures when compared to the typical stellate colonies formed in control 3D cultures. SUM159 cells and MCF7 cells had a less dramatic shift as they normally have more epithelial-like structure in 3D culture. Biomarker expression analysis revealed that adipocytes only induced a partial MET with proliferation unaffected. In addition, adipocytes had reduced lipid droplet size when co-cultured with BC cells. Thus, we found that physical interaction with adipocytes and ECM changes the mesenchymal phenotype of BC cells in a manner that could promote secondary tumor formation.

Keywords 3-dimensional culture · Co-culture system · ECM · Adipocytes · Triple negative breast cancer · Mesenchymal to epithelial transition · Metastasis

Introduction

Breast cancer is the most invasive cancer in women and metastasis is the leading cause of death from breast cancer [1, 2]. During metastasis, cancer cells can undergo an epithelial-to-mesenchymal transition (EMT) to enable migration away from the primary site, followed by a mesenchymal-to-epithelial transition (MET) to form tumours at secondary sites; both key stages in metastasis and BC progression [3].

Adipocytes have been shown to induce the expression of mesenchymal markers and promote invasiveness of BC cells, suggesting a pro-EMT function of adipocytes associated with primary tumors [4]. Adipocytes from visceral white adipose tissue (WAT) have enhanced effects on EMT of BC cells compared to those from subcutaneous WAT [5]; however, the effects of adipocytes on other aspects of BC metastasis, such as MET, are unknown.

The tumor microenvironment (TME) is one of the most important extrinsic factors that contributes to the progression of BC. It is comprised of extracellular matrix (ECM) proteins, stromal cells including adipocytes, autocrine, paracrine and endocrine secretions from associating cells, as well as the physical properties of adjacent cells or the ECM [6]. These factors can influence BC cell behaviour via biophysical or biochemical interactions and may have a compound effect on tumor growth and progression. ECM stiffness, controlled by fibre crosslinking, and the shift from laminin-rich normal breast tissue to the collagen-rich tumor environment, promotes BC progression, increases pro-inflammatory cytokine

✉ Alicia M. Vilorio-Petit
avilorio@uoguelph.ca

✉ Sherri L. Christian
sherri.christian@mun.ca

¹ Memorial University of Newfoundland, 232 Elizabeth Ave, St. Johns, NL A1B 3X9, Canada

² Department of Biomedical Sciences, Ontario Veterinary College, University of Guelph, 50 Stone Road East, Guelph, ON N1G 2W1, Canada

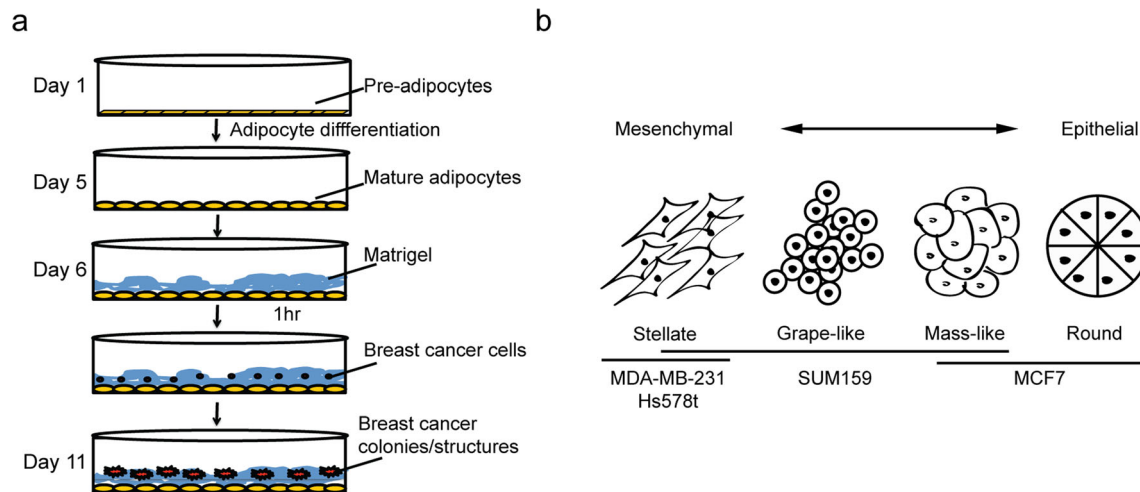


Fig. 1 Schematic representation of the 3D co-culture system. **a** Pre-adipocytes (3 T3-L1 cells) are differentiated into mature adipocytes on chamber slides for 5 days. On day 6, BC cells are overlaid in laminin-rich Matrigel and cultured in 3D for 5 days with 50% media replacement every 48 h. Immunofluorescence detection of protein markers in the BC cells and direct staining for lipid droplets in the adipocytes was performed

secretion, and decreases adipocyte lipolysis [7–9]. The ECM to adipocyte ratio can also influence cancer progression [10].

Cells in 2-dimensional (D) cell culture lack the 3D organization of cells in relation to each other or to the ECM as observed in organs and tissues in vivo [11]. In vitro 3D cell culture methods were thus developed to better mimic in vivo conditions and bridge the gap between in vitro and in vivo experiments [12–14]. Unlike cells in 2D cultures, cells grown in 3D obtain a more physiological morphology displaying aggregate structures or spheroids with prevalent cell junctions. Moreover, cells in 3D obtain phenotypic heterogeneity with varied cell proliferation rate, gene expression, and differentiation within one population [15]. Exposure to nutrients, growth factors, or drugs is also heterogeneous where cells on the outer side of spheroid are more exposed compared to cells in the inner core; more similar to in vivo conditions. In addition, cells in 3D have greater viability, less susceptibility to external factors, and show increased resistance to drug-induced stimuli [16, 17]. Lastly, both EMT or MET are better modeled in 3D culture systems compared to standard 2D culture systems [18].

on day 11. **b** A representation of the morphology of BC cells used in this study when grown in 3D culture using Matrigel. MDA-MB-231 and Hs578t cells have stellate morphology, SUM159 cells adopt grape or mass-like structures, and MCF7 cells form round/mass-like structures [12, 42]

The critical component of the in vitro 3D microenvironment is the matrix or scaffold that supports cells and allows nutrient and signal exchange among cells and with the ECM. Natural matrices such as collagen, laminin, or fibrin, as well as synthetic or artificial matrices such as Alvetex, MapTrix Hygels, or alginate, are used in in vitro 3D systems [14]. Typically, co-culture studies that interrogate the influence of other cell types are conducted in Transwell systems or direct co-culture, where physical interactions between the cells and microenvironment is missing [19, 20]. Previous studies making use of the in vitro 3D systems with co-culture with other cell types were performed using artificial matrices that need additional support such as metal and plastic inserts which are expensive and quite different from the conventional cell culture methods used in a typical lab setting [21, 22].

Therefore, we have developed an in vitro 3D co-culture system to recapitulate the in vivo interaction between BC cells, ECM, and adipocytes that is simpler and more cost-effective, all materials readily purchased commercially (Fig. 1a). As a proof of principle, here we demonstrate the use of this system to investigate the effects of adipocytes on

Table 1 Characteristics of BC cell lines used in this study

Cell line	Basal subtype	Molecular subtype	Site of origin	Histology	Morphology in 3D
MDA-MB-231	Basal B	TNBC	Pleural effusion	IDC	Mesenchymal-like [12, 32]
Hs578t	Basal B	TNBC	Primary tumor	CS	Mesenchymal-like [12, 32]
SUM159	Basal B	TNBC	Primary tumor	ANC	Round/mass-like [29]
MCF7	Luminal A	ER/PR+ HER2-	Primary tumor	IDC	Round/mass-like [30]

^a Abbreviations: IDC Invasive ductal carcinoma, CS Carcinosarcoma, ANC anaplastic carcinoma

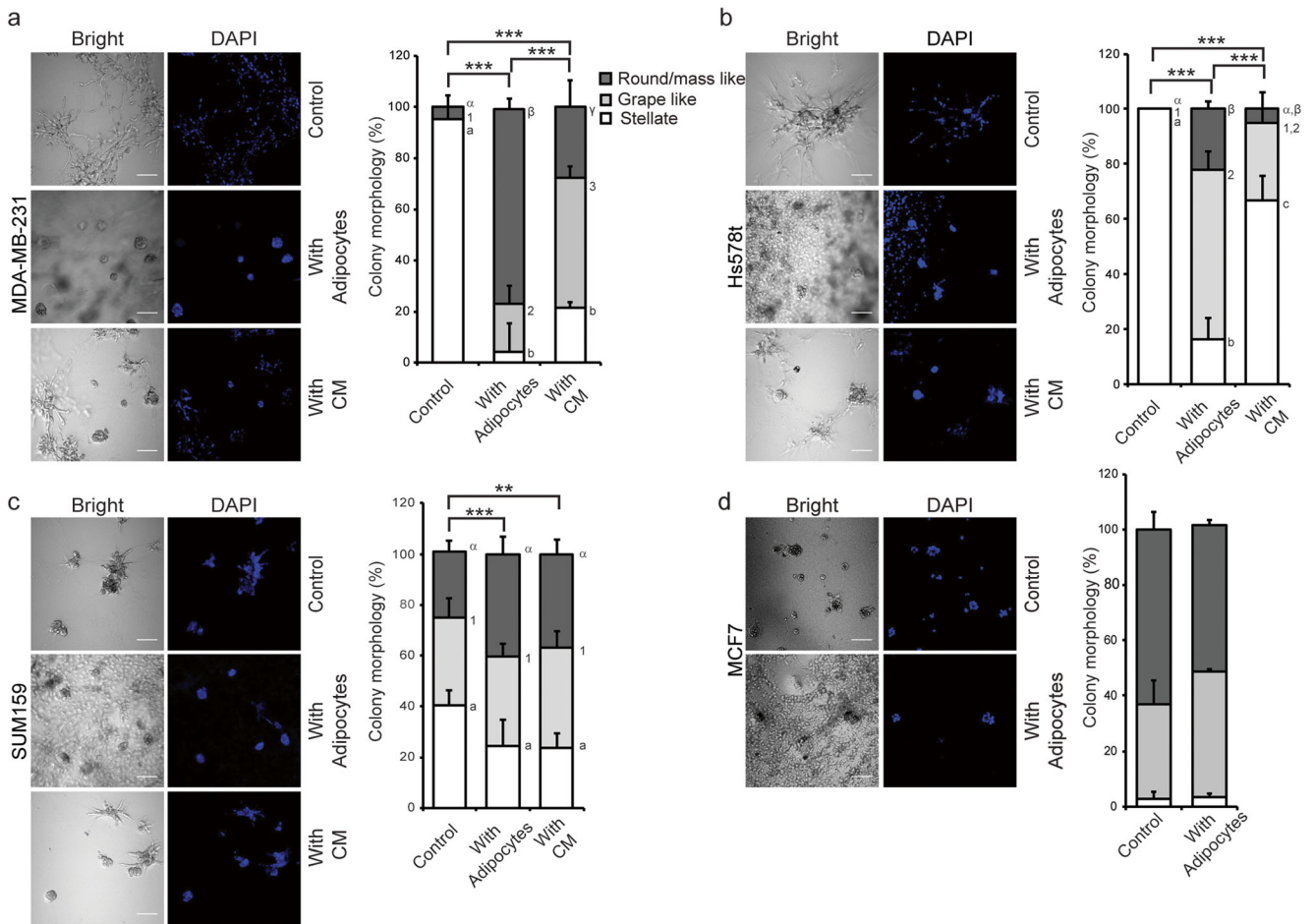


Fig. 2 Adipocytes alter the characteristic morphology of mesenchymal but not epithelial BC cell lines grown in 3D. Representative images of **a** MDA-MB-231 cells, **b** Hs578t cells, **c** SUM159 cells, and **d** MCF7 cells grown in the 3D co-culture system without adipocytes, with adipocytes, or with adipocyte conditioned media (CM). To the right of each image, the total percentage of structure shapes is shown as mean \pm SD calculated from 3 biological replicates. Overall significance of the

proportion of colony shapes between the treatments was determined by χ^2 analysis, $**P < 0.01$, $***P < 0.001$. If significant by χ^2 , differences between the conditions for each shape was determined using one-way ANOVA with Tukey HSD post hoc analysis. Different letters or symbols represent statistically different groups $a, b, c P < 0.05$ for stellate, $1, 2, 3 P < 0.05$ for grape-like, and $\alpha, \beta, \gamma, \theta P < 0.01$ for round/mass-like

BC cells, where the BC cells are grown in 3D and both cell types are exposed to ECM in the form of laminin-rich Matrigel. With this system, we analyzed protein expression in the BC cells, and lipid in the adipocytes, by fluorescent-based staining detected with confocal microscopy. We were able to detect an adipocyte-induced shift in BC colony morphology where mesenchymal MDA-MB-231 and Hs578t cells developed a round/mass colony phenotype reminiscent of an epithelial phenotype accompanied by a partial MET based on biomarker analysis, with no effect on proliferation markers. Whereas the epithelial SUM159 and MCF7 cells were not affected by adipocytes. Analysis of co-culture with pre-adipocytes revealed the effect to be dependent on adipocyte maturation and shows that the system can be expanded to any adherent cell type. We also observed that conditioned media from adipocytes (CM) had an intermediate effect on the morphology, but no effect on MET biomarkers. Lastly, we quantified lipid droplet (LD) size and number in the

adipocytes and found that LD size was reduced in the presence of MDA-MB-231, Hs578t, and MCF7 cells. In the case of MDA-MB-231 and Hs578t cells, the reduction in LD size suggests that there may be a reciprocal interaction between these BC cells and the adipocytes to actively promote the observed transition.

Materials and Methods

Cells

3T3-L1 pre-adipocytes (American Type Culture Collection, Burlington (ATCC), Burlington, ON) were maintained in high-glucose Dulbecco’s Modified Eagle Medium (DMEM) (Life Technologies Co, Burlington, ON) supplemented with 10% newborn calf serum and 1% penicillin/streptomycin (DMEM/NCS). MDA-MB-231, SUM159, Hs578t, and

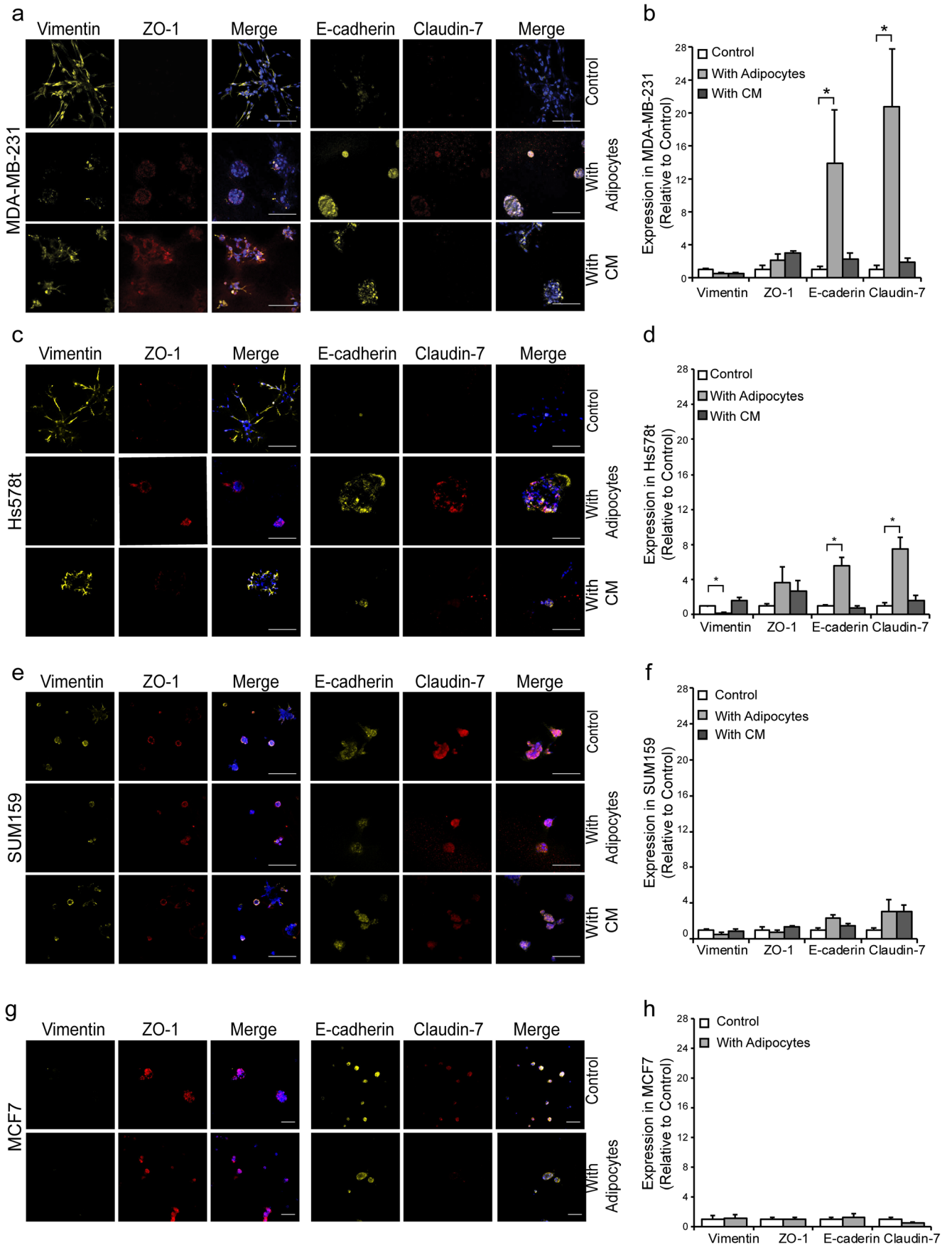


Fig. 3 Adipocytes partially enhance MET of mesenchymal BC cells in 3D culture with little to no effect on epithelial BC cells. Representative images of **a** MDA-MB-231 cells, **c** Hs578t cells, **e** SUM159 cells and **g** MCF7 cells cultured with or without adipocytes or CM and co-stained with anti-vimentin, anti-ZO-1, and DAPI (left panel), or with anti-E-cadherin, anti-Claudin-7 and DAPI (right panel) (scale bar = 50 μ m). The average protein expression in **b** MDA-MB-231 cells, **d** Hs578t cells, **f** SUM159 cells and **h** MCF7 from 5 images per replicate from different fields of view for the BC cells was normalized to DAPI and analyzed relative to control cultures. Significance was determined using Kruskal-Wallis test on ranks compared to control. * $P < 0.05$, mean \pm SD are shown from $n = 3$

MCF7 cell lines were obtained from ATCC and maintained in Roswell Park Memorial Institute (RPMI) 1640 Medium (Life Technologies) supplemented with 10% fetal bovine serum (FBS) and 1% penicillin-streptomycin. All cells were confirmed to be mycoplasma-free using the MycoAlert™ Plus Mycoplasma Detection Kit from Lonza (Basel, Switzerland). Breast cancer cell lines (Table 1) were authenticated by STR profiling by The Centre for Applied Genomics (The Hospital for Sick Children, Toronto, Canada). After thawing, all of the cell lines were used for up to 15 passages.

3T3-L1 cells were grown to confluency in 4-well chamber slides and adipogenesis was induced as previously described [23]. Briefly, pre-adipocytes were grown to confluency and then initiation media containing 0.5 mM 3-isobutyl-1-methylxanthine and 1 μ M Dexamethasone (Millipore, Darmstadt, Germany) in DMEM supplemented with 10% FBS and 1% penicillin/streptomycin (DMEM/FBS) was added to the cells 48 h post-confluency. Initiation media was replaced with progression media (10 μ g/ml insulin (Sigma-Aldrich, St. Louis, MI, USA) in DMEM/FBS) after 48 h followed by replacement with DMEM/FBS 48 h later. To obtain conditioned media (CM), adipocytes were differentiated for 5 days as described above, the maintenance media was replaced by co-culture media (mammary epithelial basal media: MEBM, Promo Cell, Heidelberg, Germany) containing epidermal growth factor (10 ng/ml), insulin (5 μ g/ml), hydrocortisone (0.5 μ g/ml), bovine pituitary extract (0.4%) and 2% Matrigel), and collected 48 h after Matrigel was overlaid. Media was refreshed and CM was collected again 48 h later. CM was mixed 1:1 with fresh media and added to the breast cancer cells overlaid on Matrigel on Day 6 and 8. Adipocyte and CM co-cultures were maintained for 5 days, and pre-adipocyte co-cultures maintained for 4 days, after plating BC cells on Matrigel. Note that there were no differences in colony structure or protein expression in breast cancer cells cultured on Matrigel for 4 or 5 days in the control cultures.

3D Co-culture

We modified the 3D culture method initially developed by Dr. Mina Bissell [12] and adapted by Debnath et al. [24], as

follows (Fig. 1a). 3T3-L1 cells were differentiated for 5 days, at which point the lipid droplets were clearly observable in >60% of the cells. On day 6, 110 μ l of Matrigel (a basement membrane matrix growth factor reduced, phenol red free, Cat# 356231, 9.1 mg/ml, BD Bioscience) was overlaid on top of mature adipocytes, or empty wells of a 4-well chamber slide and allowed to set for 1 h (Fig. 1a). MDA-MB-231/MCF7 (13,500 cells/450 μ l), SUM159 (11,250 cells/450 μ l), or Hs578t (18,000 cells/450 μ l) were overlaid and incubated with co-culture media. BC cells were grown for an additional 4–5 days to allow colony formation. For the pre-adipocyte co-culture, pre-adipocytes were plated on day 5, allowed to undergo growth arrest for 48 h, and then Matrigel and breast cancer cells were overlaid on day 7.

Immunofluorescence (IF)

Cells were fixed with 4% paraformaldehyde for 20 min at room temperature (RT), followed by permeabilization in 1X PBS containing 0.5% Triton X-100 for 10 min at 4 $^{\circ}$ C, then washed 3 times with PBS-glycine (100 mM glycine in 1X PBS) and blocked with 10% donkey serum in IF buffer (0.1% BSA, 0.2% Triton X-100, 0.05% Tween 20, 1X PBS) for 1 h at RT. Primary antibodies were diluted in blocking buffer, incubated overnight at 4 $^{\circ}$ C and detected with appropriate secondary antibodies. Before and after secondary staining cells were washed 3 times with IF buffer. Co-cultures were then stained with DAPI (Life technologies) and/or BODIPY 493/503 (Life Technologies) for LD detection for 25 min at RT, then washed 1 time with 1X PBS. The chambers were separated from the slide according to manufacturer's protocol and any excess 1X PBS was gently removed. An even bead of silicone sealant (GE, Boston, MA, USA) was applied around the Matrigel layer to avoid compression of co-cultures by coverslips. Prolong Gold (Life technologies) was used for mounting slides and placed in dark at RT to dry overnight. The slides were imaged using the 20X and 40X objective with the Nikon A1 confocal microscope with NIS elements imaging software (Nikon Inc, Tokyo, Japan).

Primary antibodies and dilutions used were as follows: vimentin (1:200; Cat #V2258; Sigma-Aldrich, St. Louis, MO, USA), ZO-1 (1:50; Cat #SC8146; SantaCruz Biotechnology Inc., Santa Cruz, CA, USA), E-cadherin (1:200; Cat #610181; BD Biosciences, Franklin Lakes, NJ, USA), Claudin7 (1:200; Cat #AB27487; Abcam, Cambridge, UK), CD24 (1:100; Cat #NBP1-46390; Novus Biologicals, Littleton, CO, USA), CD44 (1:25; Cat #M708201-2; Dako), and Ki67 (1:100; Cat #M724029-1; Dako, Denmark). Secondary antibodies used were AlexaFluor-647 anti-goat (Cat #705-605-003; Jackson ImmunoResearch laboratories, West grove, PA, USA), AlexaFluor-647 anti-rabbit (Cat #711-605-152; Jackson ImmunoResearch laboratories), and DyLight 594 anti-mouse (NBP1-75617; Novus biologicals).

Image Analyses

Colony morphologies were assessed by analysis of circularity using ImageJ v. 1.48 [25]. Structures present in three images per replicate (minimum 10 structures per replicate) were traced manually and the circularity measurement was obtained. A circularity value >0.7 was classified as round/mass-like, $0.7-0.2$ was classified as grape-like, and <0.2 was classified as stellate (Fig. 1b).

Protein expression was analyzed using ImageJ by measuring the intensity of fluorescence of the whole image. Integrated density (IntDen) was determined to capture the total fluorescence of each marker. Background was subtracted by taking measurements of selected areas where cells were absent as observed from the respective bright field images. The total fluorescence intensity of each marker was determined by normalizing IntDen of each marker to IntDen of DAPI and then the relative IntDen values of each marker per condition was determined relative to the control.

ImageJ was used to analyze the number and size of LDs [26] from 5 independent fields of view per biological replicate where images from 5 different depths (Z-stack) were condensed to form a single 2D composite image of all BODIPY 493/503 stained LD. The composite image was converted to an 8-bit binary image followed automatic threshold adjustment and then a watershed-based separation of closely spaced LD applied before calculation of LD area and number.

Statistical Analysis

Statistical analysis was performed in R v.3.3 [27] accessed through RStudio [28]. Significant differences in lipid droplet area distributions between each experimental condition were determined using the Kolmogorov-Smirnov test. Significant differences in lipid droplet number was determined by Student's *t* test. Differences in the distribution of colony shape was determined by χ^2 analysis between control and experimental conditions. Significant differences in specific colony shape was determined using a 4 X 3 between subjects factorial ANOVA, followed by one-way ANOVAs and Tukey HSD post-hoc analysis within each shape between conditions. Differences were considered statistically significant at $P < 0.05$.

Results

Adipocytes Cause Mesenchymal BC Cells Grown in 3D to Adopt More Epithelial Type Structures with Little Effect on Epithelial BC Cells

We first determined if co-culturing adipocytes with the mesenchymal or partly mesenchymal cells, MDA-MB-231,

Hs578t and SUM159 cells or epithelial MCF7 cells grown in 3D affected the structure of the BC cell lines. We found that adipocytes significantly increased the number of grape-like, and round/mass-like structures formed by MDA-MB-231 and Hs578t cells (Fig. 2a and b). SUM159 cells have a stellate morphology in 2D culture [29] that changes to a mixed morphology in 3D culture with more round/grape like structures, as compared to MDA-MB-231 and Hs578t cells for example. This mixed morphology was minimally affected by co-culture with adipocytes (Fig. 2c). MCF7 cells form a cobblestone-like morphology in 2D culture that changes to round/mass-like morphology in 3D culture [30]. We found that adipocytes had no significant effect on the morphology of MCF7 cells in the co-culture system (Fig. 2d).

We next analyzed if these changes are induced by a soluble mediator released by adipocytes cultured with ECM or via a physical interaction with the adipocytes. We focused only on cell lines where an adipocyte-induced effect was seen. We found that adipocyte CM induced the loss of stellate and the gain of grape-like structures in MDA-MB-231 and Hs578t cultures, along with an intermediate and non-significant increase in round/mass-like structures (Fig. 2a and b). Similar to adipocytes, CM had no substantial effect on the specific colony morphology of SUM159 cells in 3D cultures (Fig. 2c).

Adipocytes have a Partial Effect on Expression of Mesenchymal to Epithelial Transition Markers in MDA-MB-231 and Hs578t Cells

We next assessed the use of IF to specifically detect the expression of EMT protein markers in the 3D co-cultures. We examined expression of Claudin-7, ZO-1, and E-cadherin, which are epithelial markers, and vimentin, a mesenchymal marker, in the presence and absence of adipocyte co-culture [31].

As expected, the MDA-MB-231 and Hs578t cells grown in the absence of adipocytes had high vimentin and low E-cadherin, ZO-1 and Claudin-7 expression. MCF7 cells had high expression of epithelial markers and low expression of vimentin, whereas, SUM159 cells had high E-cadherin, ZO-1, Claudin-7 and vimentin expression. We observed that adipocytes induced a significant gain in the expression of both E-cadherin and Claudin-7 in MDA-MB-231 and Hs578t cells (Fig. 3a–d). In addition, Hs578t showed a significant reduction in vimentin expression (Fig. 3c and d). Significant changes to ZO-1 were not observed in any of the cell lines when co-cultured with adipocytes. EMT markers were not significantly altered in either SUM159 or MCF7 cells (Fig. 3e–h). When cultured with adipocyte CM, no significant changes in EMT biomarker expression were observed in any of the cells (Fig. 3). Together, these data suggest that mature adipocytes promote a partial MET in mesenchymal MDA-MB-231 and Hs578t cells that is not fully recapitulated by soluble mediator.

Adipocytes have a Partial Effect on BC Stem Cell Biomarkers but no Effect on Proliferation Markers

Similarly, we analyzed the effect of adipocytes on the presence of BC stem cells (BCSCs) as indicated by CD44^{high}/CD24^{low} expression, biomarkers known to correlate with the abundance of BCSCs in cell culture [32]. We found that adipocytes and adipocyte CM increased CD24 levels in MDA-MB-231 cells with no change

observed in any of the other cell lines (Fig. 4). Thus, mature adipocytes induce the gain of CD24 but this is not likely to be associated with the BCSC phenotype. Moreover, the CM-induced increase of CD24 expression indicates that a soluble factor promotes this increase.

We next analyzed the effect of adipocytes on expression of the Ki67 proliferation marker. We found that there was no significant change in Ki67 expression levels in any of the co-culture conditions tested (Fig. 4).

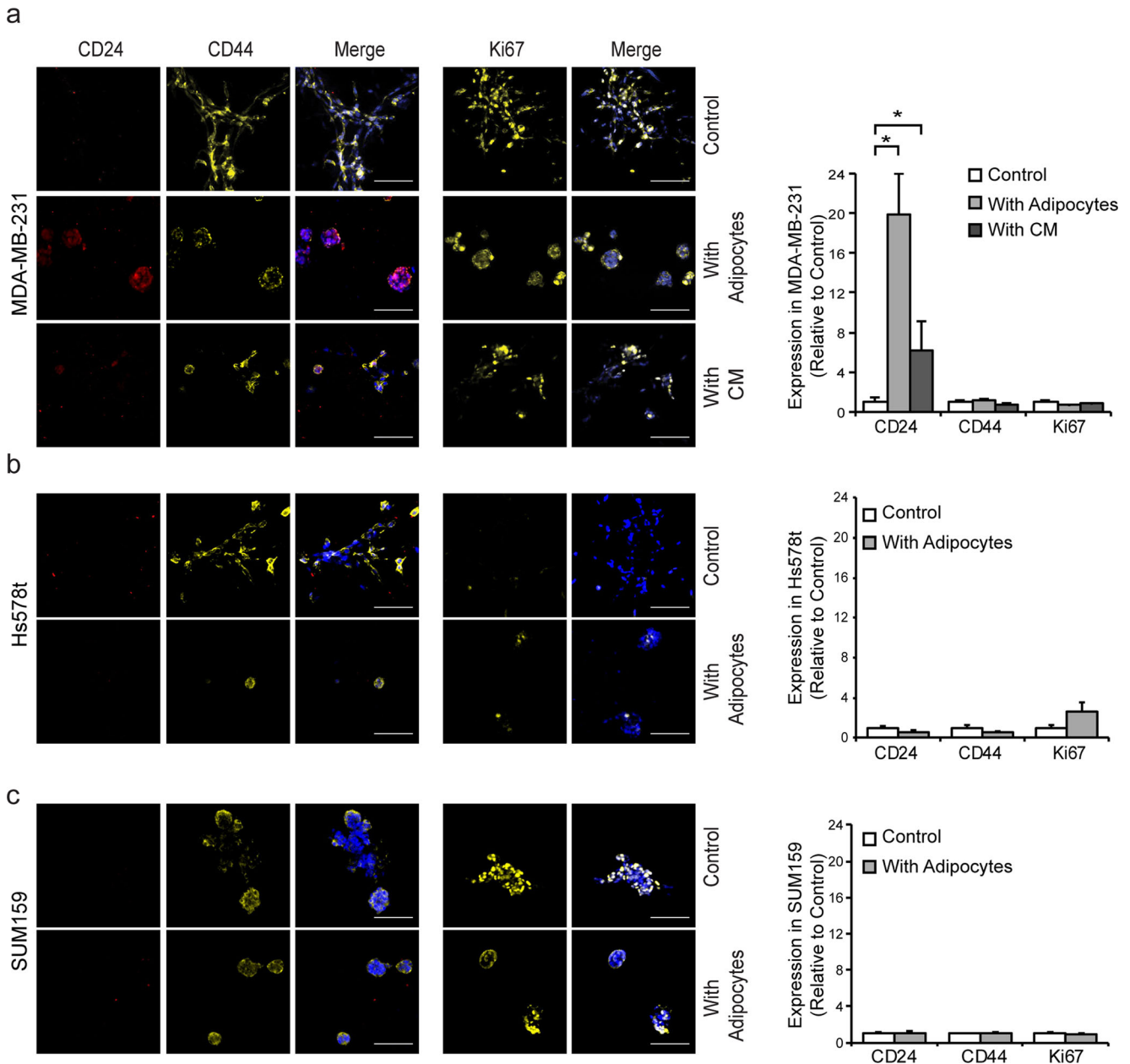
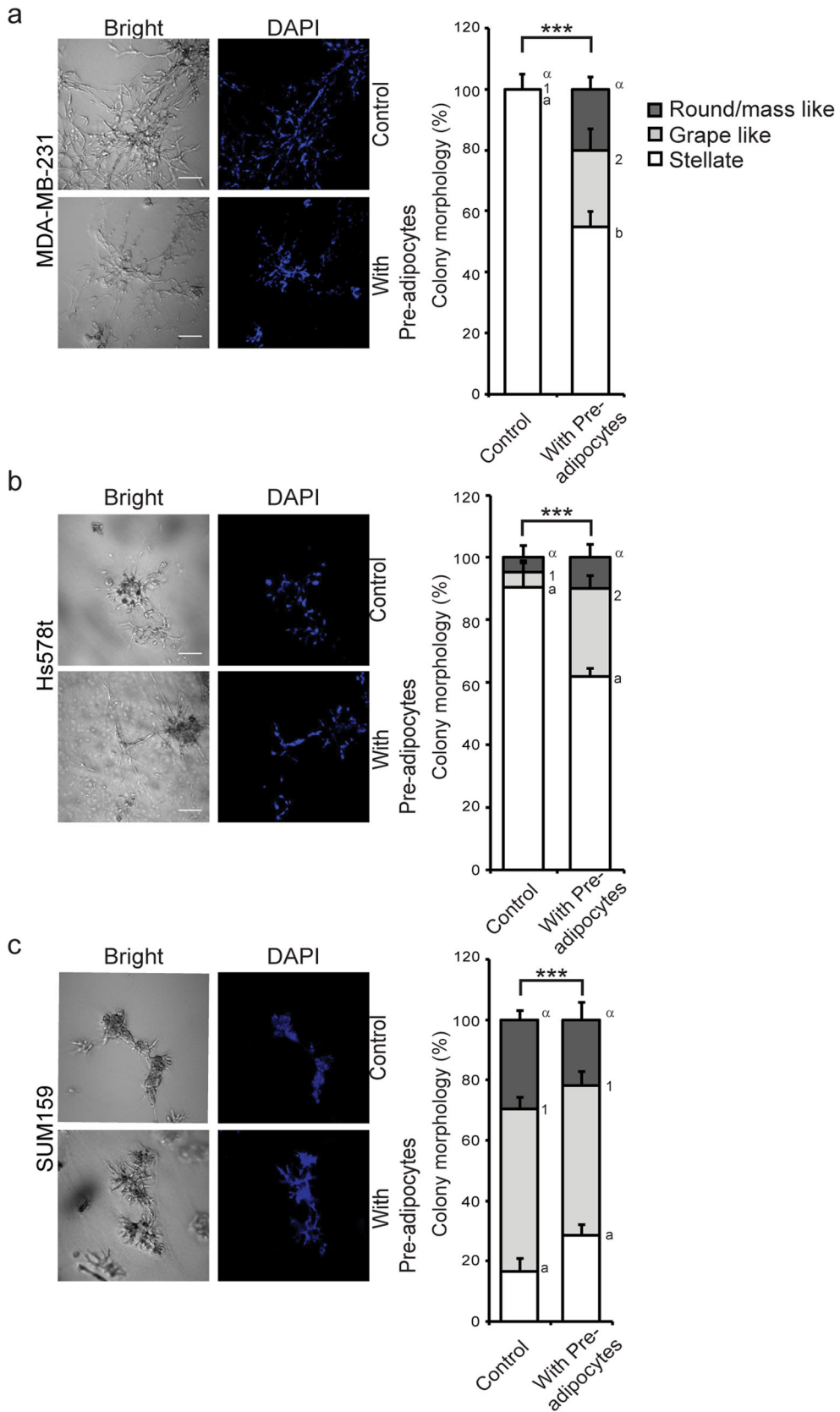


Fig. 4 Adipocytes increase CD24 in MDA-MB-21 cells with no effect on CD44 or the Ki67 proliferation marker in any cell line. Representative images of **a** MDA-MB-231 cells, **b** Hs578t cells and **c** SUM159 cells in the presence or absence of adipocytes and conditioned media co-stained with anti-CD24, anti-CD44, and DAPI (left panel), or co-stained with anti-Ki67 and DAPI (right panel) (scale bar = 50 μm). To

the right of each image, the average protein expression of 5 images per replicate from different fields of view for the BC cells was normalized to DAPI and analyzed relative to control cultures. Significance was determined using Kruskal-Wallis test on ranks compared to control. * $P < 0.05$, $n = 3$



◀ **Fig. 5 Pre-adipocytes have a partial effect on morphology of BC cells.** Representative images of **a** MDA-MB-231 cells, **b** Hs578t cells and **c** SUM159 cells grown in the 3D co-culture system in the presence or absence of pre-adipocytes (Scale bar = 100 μm). To the right of each image, the total percentage of structure shapes as mean \pm SD are shown from 3 biological replicates. Overall significance of the proportion of colony shapes between the treatments was determined by χ^2 analysis, $**P < 0.01$, $***P < 0.001$. If significant by χ^2 , differences between the conditions for each shape was determined using one-way ANOVA with Tukey HSD post hoc analysis. Different letters or symbols represent statistically different groups $^{a,b,c}P < 0.05$ for stellate, $^{1,2,3}P < 0.05$ for grape-like, and $^{\alpha,\beta,\gamma,\theta}P < 0.01$ for round/mass-like

The Change in Morphology or MET of Mesenchymal BC Cells is Specific to Mature Adipocytes

To determine if we could apply this model to differentiate the effects caused by other cell types on the BC cell lines, we examined the effect of undifferentiated pre-adipocytes co-cultured with BC cell lines, focusing on cell lines that were affected by adipocytes. We found that incubation with undifferentiated pre-adipocytes had a partial effect on the morphology of the cell lines that was much less dramatic than seen with mature adipocytes (Fig. 5). Similarly, we analyzed EMT markers expression in the BC cell lines in presence of pre-adipocytes and found no effect on any of the cell lines (Fig. 6). Since MDA-MB-231 were the only cells with changes to CD24, we analyzed the effect of pre-adipocytes on this line only for stemness and proliferation makers and found that pre-adipocytes caused no significant change in CD24, CD44 or Ki67 expression (Fig. 6g and h).

LD Size is Decreased in 3D Co-cultures

To determine if we were able to analyze the adipocytes, which are located beneath the Matrigel layer, we stained adipocyte LDs with the fluorescent lipophilic dye BODIPY 493/503. Using confocal microscopy, we were clearly able to image and analyze both the size and number of LDs. We observed that the number of LDs did not significantly change in the presence of any of BC cell line (MDA-MB-231: $P = 0.142$, Hs578t: $P = 0.429$, SUM159: $P = 0.999$, MCF7: $P = 0.052$) (Fig. 7b). However, adipocytes displayed an altered distribution of LDs sizes in response to co-culture with any of the BC cell lines (MDA-MB-231: $P < 0.0001$, Hs578t: $P = 0.00812$, SUM159: $P < 0.0001$, MCF7: $P < 0.0001$) (Fig. 7c). MDA-MB-231 cells caused a decrease in the number of LDs in all bins 100 μm^2 or greater. Hs578t cells had a less dramatic effect with a reduction in LDs of 250 μm^2 or greater. Even MCF7 cells, that were themselves not affected by adipocyte co-culture, caused a reduction in LDs 100 μm^2 and greater. In contrast, we observed an increase in the frequency of LDs greater than 150 μm^2 with SUM159 co-culture.

Discussion

Here, we report on the development and use of a 3D co-culture system to allow the evaluation of interactions between two different cell types where both cell types are in contact with the ECM. The system we describe does not require custom equipment, scaffolding, or other techniques inaccessible to modern cellular biology labs. The system has the noted benefit of allowing assessment of epithelial and mesenchymal states that are particularly vulnerable to differences in the 2D vs. 3D environment [12].

We developed this 3D co-culture system to enable the analysis of proteins or lipid of interest by IF and confocal imaging. Here, we focused on analysis of the EMT status of BC cell lines using human specific antibodies. We have used adipocytes and laminin-rich ECM in this study, however, this method could easily be modified to analyse interaction with other types of ECM, stromal cells, or primary cells in the presence of biological modifiers. It has been shown that BC cells isolated from 3D culture can maintain their characteristics for up to 8 weeks, thus, allowing for further assessment of changes to the migration and invasion ability induced by co-culture [33, 34].

It is important to note that the major technical limitation for imaging the 3D co-cultures is obtaining high resolution images due to the thickness of the sample, which limits the ability to obtain well focused images, particularly with higher magnification objectives with limited focal length. It is possible that this limitation could be overcome by formalin fixed, paraffin embedded - immunofluorescence or immunohistochemistry (FFPE-IF/IHC) techniques, which would create thinner physical slices. However, the additional processing and need for compatible antibodies adds a different set of caveats. [35]. More accurate quantification of protein levels than shown here could theoretically be accomplished after isolation and cell lysis followed by detection using western blot as previously described [12]. However, in order to obtain sufficient protein quantity, the size of the chambers would need to be increased, which is accompanied by a significant increase in cost. Excess protein from the added ECM can also introduce challenges in ensuring equal loading of the cell-specific proteins.

To demonstrate the utility of this method, we analyzed the effect of adipocytes on the 3D morphology of mesenchymal and epithelial BC cell lines. Interestingly, and in contrast to a previous report [4], we found that adipocytes promoted a partial MET in mesenchymal BC cells, as evidenced by the changes to colony morphology and changes in expression of Claudin-7 and E-cadherin in MDA-MB-231 and Hs578t cells and vimentin in Hs578t cells. In contrast, SUM159, which are more epithelial in 3D-culture cells, did not show any significant changes to colony morphology or EMT marker expression. Surprisingly, MCF7 cells showed no change in their

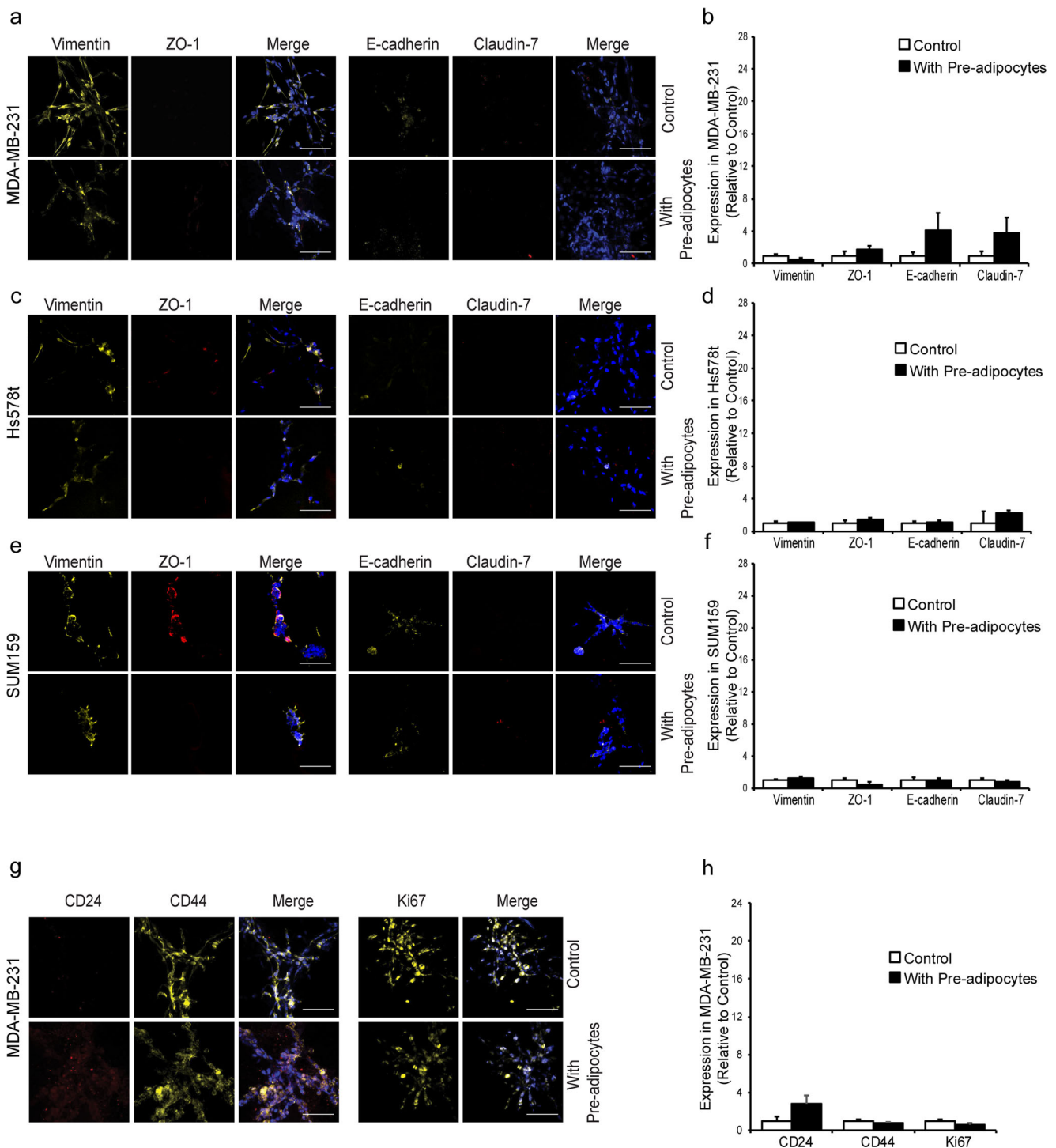


Fig. 6 Pre-adipocytes have no effect on MET or on stemness markers of BC cells. Representative images of **a** MDA-MB-231 cells, **c** Hs578t cells and **e** SUM159 cells cultured with or without pre-adipocytes, and co-stained with anti-vimentin, anti-ZO-1, and DAPI (left panel), or co-stained with anti-E-cadherin, anti-Claudin-7 and DAPI (right panel). **b, d, f, h** The average protein expression of 5 images per replicate from different fields of view for the TNBC cells was normalized to DAPI

and analyzed relative to control cultures. Significance was determined using Kruskal-Wallis test on ranks compared to control. $n = 3$. Representative images of **g** MDA-MB-231 cells, grown in 3D culture in the absence or presence of pre-adipocytes, and then co-stained with anti-CD24, anti-CD44, and DAPI (left panel), or co-stained with anti-Ki67 and DAPI (right panel), (scale bar = 50 μm)

EMT status in presence of adipocytes, unlike what was seen in Transwell culture studies [4]. This suggests that physical

interactions of BC and adipocytes with the ECM has an essential role in the biology of EMT and MET of BC cells.

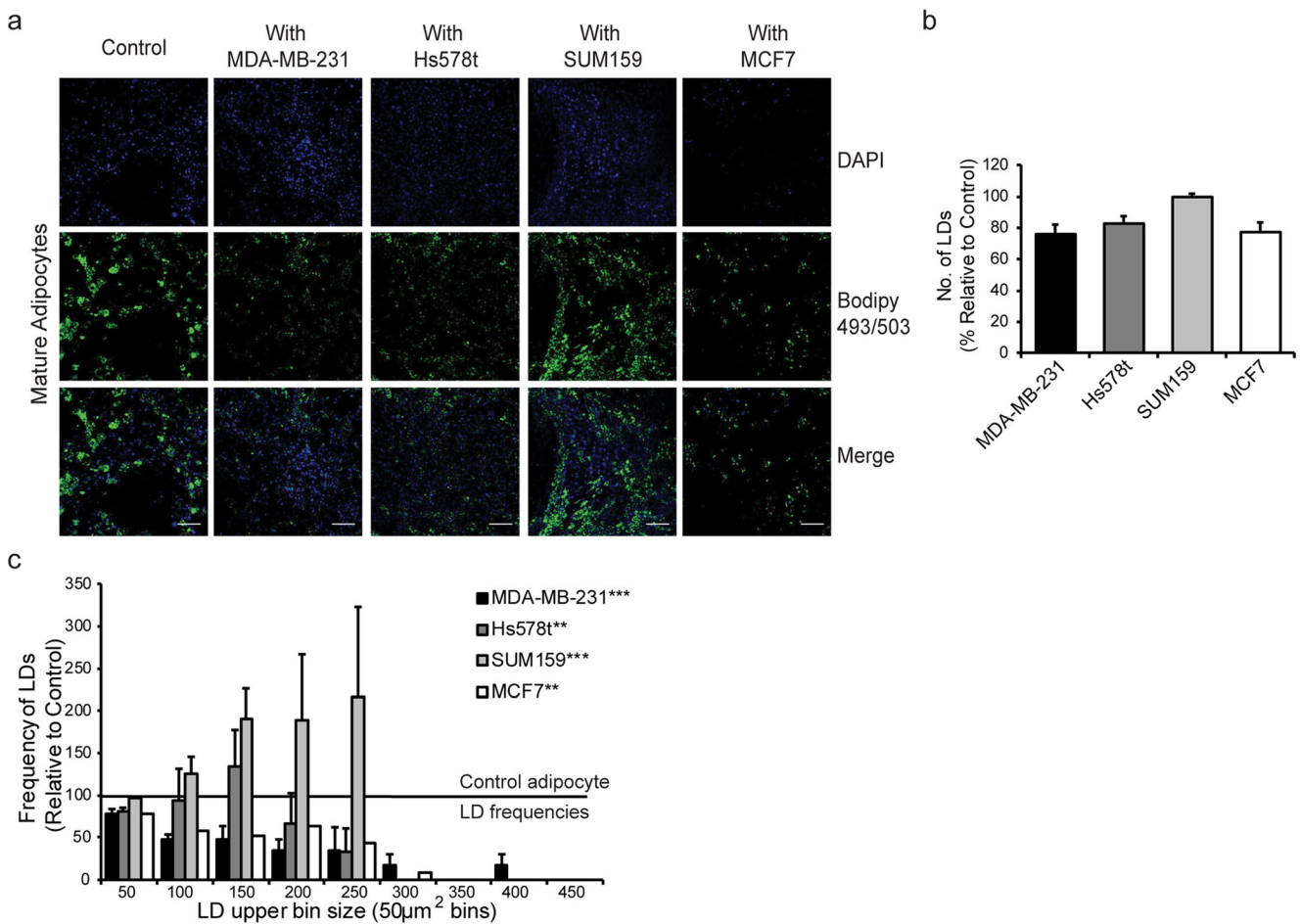


Fig. 7 Co-culture with BC cells decreases the size but not number of LD present in mature adipocytes. **a** Representative images of adipocyte LDs co-stained with Bodipy 493/503 and DAPI in the presence and absence of BC cells in the 3D co-culture system. (scale bar = 100 µm), *n* = 3. **b** Number of LDs analyzed from 5 random fields of view per

replicate shown as mean ± SD. Significant differences were determined using Students *t*-test, *n* = 3. **c** Distributions of areas binned by 50 µm². Significance was determined using Kolmogorov-Smirnov test, *n* = 3, ***P* < 0.01, ****P* < 0.001, mean ± SD are shown from *n* = 3. Note: error bars for MCF7 are too small to be visible

To determine if this method can differentiate the effect of physical interactions vs. soluble mediators, we examined if CM could recapitulate the adipocyte-induced effects. We found that CM was sufficient to change the morphology of MDA-MB-231 and Hs578t cells to an epithelial-like colony shape but did not induce similar MET-like changes in biomarker expression. It must be noted that the CM was diluted by 50% at each media change to ensure replenishment of nutrients for cell survival. Thus, the reduced concentration of soluble mediators may have caused this partial effect. Alternatively, constant exposure of a mediator or the physical presence of mature adipocytes may be necessary to surpass a signaling threshold in the BC cells. A partial change that was even less dramatic was observed in the presence of pre-adipocytes suggesting that the mediator is more abundant or effective when originating from adipocytes.

Here, we have used the 3T3-L1 mouse pre-adipocyte cell line to be confident of detecting only human proteins

expressed on the human BC cell lines during imaging by making use of species-specific antibodies. Furthermore, specific detection of mouse proteins would ensure identification of the adipocyte mediator in future studies. However, to establish the biological significance of this interaction, it will be necessary to determine if the same mediator is secreted by human adipocytes; a limitation of the current study. Preliminary data suggests that primary adipocytes from humans and mice may have a similar effect of promoting a MET-like change in MDA-MB-231 cells, however, this system will require significant optimizations as initial experiments indicate that the media used for primary cell differentiation is incompatible with the 3D culture and vice versa. Regardless, identification of the factor secreted by mouse adipocytes might reveal a receptor or target on the BC cells that actively promotes the MET-like changes, which could potentially be targeted in the future.

In obese patients, increases in the number of adipocytes also increases the complexity of the interactions

between the TME, adipocytes and BC, which can contribute to BC progression [36]. Moreover, increased adiposity in the bone marrow has been shown to lead to metastasis from ovarian and prostate cancers [37, 38]. However, it is not known whether the composition and/or mechanical properties of the ECM at sites of metastasis are similar to that used in the present study. Future work will be required to elucidate the precise mechanism(s) contributed by adipocytes to BC metastasis at specific sites, the role of the ECM in these processes, and any effect of obesity on the same.

Differences in LD size suggests that lipid in the adipocytes could be mobilized by MDA-MB-231, Hs578t cells, or MCF7, which may provide energy in the form of free fatty acids taken up by BC cells to fuel cellular processes. Increased lipolysis by adipocytes in the BC microenvironment and increased expression of fatty acid binding proteins in ovarian cancer, combined with studies showing high levels of oxidative phosphorylation in BC cells, supports this possibility [39, 40]. Alternatively, adipocytes can affect BC cells via the increased secretion of leptin, IL-6, TNF, and VEGF, as observed in obese patients [41]. In SUM159 cells, there was no decrease in LD size which may also explain the lack of change to the phenotype of these cells, however it remains to be determined why MCF7 cell phenotype is unaffected by adipocytes yet LD size is decreased.

Here, we demonstrate the use of a novel, straightforward, and accessible 3D co-culture method to show that adipocytes can promote a MET-like change in mesenchymal TNBC cells. This work provides more insight into relationship between high adiposity and metastasis to bone or other sites with adipocyte abundance. Future work using this model to identify the mechanism(s) underlying this process may enable identification of better therapeutic targets for metastatic BC.

Funding Funding provided to SLC by the Memorial University of Newfoundland (210525), a New Investigator Award from the Beatrice Hunter Cancer Research Institute (207939), and the Cancer Research Society (22130). An NSERC Discovery Grant to AVP provided funding for optimization of the 3D culture model (RGPIN-2017-3977). NKP was supported by a trainee award and a Skills Acquisition Program award from the Beatrice Hunter Cancer Research Institute with funds provided by The Terry Fox Strategic Health Research Training Program in Cancer Research at CIHR and by Memorial University of Newfoundland.

Compliance with Ethical Standards

Conflict of Interest The authors declare that they have no conflicts of interest.

Ethical Approval This article does not contain any studies with human participants or animals.

References

1. Canadian Cancer Statistics 2017. Canadian Cancer Society's Advisory Committee on cancer statistics. Can Cancer Soc. 2017. <https://cancer.ca/canadian-cancer-statistics-2017-EN.pdf>. Accessed 3 March 2018.
2. Jin X, Mu P. Targeting breast cancer metastasis. *Breast Cancer (Auckl)*. 2015;9:23–34. <https://doi.org/10.4137/BCBCR.S25460>.
3. Chaffer CL, Weinberg RA. A perspective on cancer cell metastasis. *Science*. 2011;331:1559–64. <https://doi.org/10.1126/science.1203543>.
4. Lee Y, Jung WH, Koo JS. Adipocytes can induce epithelial-mesenchymal transition in breast cancer cells. *Breast Cancer Res Treat*. 2015;153:323–35. <https://doi.org/10.1007/s10549-015-3550-9>.
5. Ritter A, Friemel A, Fornoff F, Adjan M, Solbach C, Yuan J, et al. Characterization of adipose-derived stem cells from subcutaneous and visceral adipose tissues and their function in breast cancer cells. *Oncotarget*. 2015;6:34475–93. <https://doi.org/10.18632/oncotarget.5922>.
6. Place AE, Jin Huh S, Polyak K. The microenvironment in breast cancer progression: biology and implications for treatment. *Breast Cancer Res*. 2011;13:227. <https://doi.org/10.1186/bcr2912>.
7. Howlett AR, Bissell MJ. The influence of tissue microenvironment (stroma and extracellular matrix) on the development and function of mammary epithelium. *Epithelial Cell Biol*. 1993;2:79–89.
8. Chaudhuri O, Koshy ST, Branco da Cunha C, Shin JW, Verbeke CS, Allison KH, et al. Extracellular matrix stiffness and composition jointly regulate the induction of malignant phenotypes in mammary epithelium. *Nat Mater*. 2014;13:970–8. <https://doi.org/10.1038/nmat4009>.
9. Pellegrinelli V, Heuvingh J, du Roure O, Rouault C, Devulder A, Klein C, et al. Human adipocyte function is impacted by mechanical cues. *J Pathol*. 2014;233:183–95. <https://doi.org/10.1002/path.4347>.
10. Seo BR, Bhardwaj P, Choi S, Gonzalez J, Andresen Eguiluz RC, Wang K, et al. Obesity-dependent changes in interstitial ECM mechanics promote breast tumorigenesis. *Sci Transl Med*. 2015;7:301ra130. <https://doi.org/10.1126/scitranslmed.3010467>.
11. Duval K, Grover H, Han L-H, Mou Y, Pegoraro AF, Fredberg J, et al. Modeling physiological events in 2D vs. 3D cell culture. *Physiology (Bethesda)*. 2017;32:266–77. <https://doi.org/10.1152/physiol.00036.2016>.
12. Kenny PA, Lee GY, Myers CA, Neve RM, Semeiks JR, Spellman PT, et al. The morphologies of breast cancer cell lines in three-dimensional assays correlate with their profiles of gene expression. *Mol Oncol*. 2007;1:84–96. <https://doi.org/10.1016/j.molonc.2007.02.004>.
13. Ravi M, Paramesh V, Kaviya SR, Anuradha E, Solomon FDP. 3D cell culture systems: advantages and applications. *J Cell Physiol*. 2015;230:16–26. <https://doi.org/10.1002/jcp.24683>.
14. Baker BM, Chen CS. Deconstructing the third dimension: how 3D culture microenvironments alter cellular cues. *J Cell Sci*. 2012;125:3015–24. <https://doi.org/10.1242/jcs.079509>.
15. Luca AC, Mersch S, Deenen R, Schmidt S, Messner I, Schäfer KL, et al. Impact of the 3D microenvironment on phenotype, gene expression, and EGFR inhibition of colorectal cancer cell lines. *PLoS One*. 2013;8:e59689. <https://doi.org/10.1371/journal.pone.0059689>.
16. Ajjitawi OS, Li D, Xiao Y, Zhang D, Ramachandran K, Stehno-Bittel L, et al. A novel three-dimensional stromal-based model for in vitro chemotherapy sensitivity testing of leukemia cells. *Leuk Lymphoma*. 2014;55:378–91. <https://doi.org/10.3109/10428194.2013.793323>.

17. Fang Y, Eglen RM. Three-dimensional cell cultures in drug discovery and development. *SLAS Discov*. 2017;22:456–72. <https://doi.org/10.1177/1087057117696795>.
18. Bidarra SJ, Oliveira P, Rocha S, Saraiva DP, Oliveira C, Barrias CC. A 3D in vitro model to explore the inter-conversion between epithelial and mesenchymal states during EMT and its reversion. *Sci Rep*. 2016;6:27072. <https://doi.org/10.1038/srep27072>.
19. Salameh TS, Le TT, Nichols MB, et al. An ex vivo co-culture model system to evaluate stromal-epithelial interactions in breast cancer. *Int J Cancer*. 2013;132:288–96. <https://doi.org/10.1002/ijc.27672>.
20. Herroon MK, Diedrich JD, Podgorski I. New 3D-culture approaches to study interactions of bone marrow adipocytes with metastatic prostate cancer cells. *Front Endocrinol (Lausanne)*. 2016;7:84. <https://doi.org/10.3389/fendo.2016.00084>.
21. Kimlin LC, Casagrande G, Virador VM. In vitro three-dimensional (3D) models in cancer research: an update. *Mol Carcinog*. 2013;52:167–82. <https://doi.org/10.1002/mc.21844>.
22. Huang J, Duran A, Reina-Campos M, Valencia T, Castilla EA, Müller TD, et al. Adipocyte p62/SQSTM1 suppresses tumorigenesis through opposite regulations of metabolism in adipose tissue and tumor. *Cancer Cell*. 2018;33:770–784.e6. <https://doi.org/10.1016/j.ccell.2018.03.001>.
23. Smith NC, Fairbridge NA, Pallegar NK, Christian SL. Dynamic upregulation of CD24 in pre-adipocytes promotes adipogenesis. *Adipocyte*. 2014;4:89–100. <https://doi.org/10.4161/21623945.2014.985015>.
24. Debnath J, Muthuswamy SK, Brugge JS. Morphogenesis and oncogenesis of MCF-10A mammary epithelial acini grown in three-dimensional basement membrane cultures. *Methods*. 2003;30:256–68.
25. Schneider CA, Rasband WS, Eliceiri KW. NIH image to ImageJ: 25 years of image analysis. *Nat Methods*. 2012;9:671–5.
26. Grishagin IV. Automatic cell counting with ImageJ. *Anal Biochem*. 2015;473:63–5. <https://doi.org/10.1016/j.ab.2014.12.007>.
27. R Core Development Team. R: a language and environment for statistical computing. Vienna: R Foundation for Statistical Computing; 2015.
28. RStudio Team. RStudio: integrated development for R. Boston: RStudio, Inc.; 2015.
29. Barnabas N, Cohen D. Phenotypic and molecular characterization of MCF10DCIS and SUM breast cancer cell lines. *Int J Breast Cancer*. 2013;2013:1–16. <https://doi.org/10.1155/2013/872743>.
30. Lee GY, Kenny PA, Lee EH, Bissell MJ. Three-dimensional culture models of normal and malignant breast epithelial cells. *Nat Methods*. 2007;4:359–65. <https://doi.org/10.1038/nmeth1015>.
31. Lamouille S, Xu J, Derynck R. Molecular mechanisms of epithelial-mesenchymal transition. *Nat Rev Mol Cell Biol*. 2014;15:178–96. <https://doi.org/10.1038/nrm3758>.
32. Lehmann BD, Bauer JA, Chen X, Sanders ME, Chakravarthy AB, Shyr Y, et al. Identification of human triple-negative breast cancer subtypes and preclinical models for selection of targeted therapies. *J Clin Invest*. 2011;121:2750–67. <https://doi.org/10.1172/JCI45014>.
33. Xu K, Buchsbaum RJ. Isolation of mammary epithelial cells from three-dimensional mixed-cell spheroid co-culture. *J Vis Exp*. 2012. <https://doi.org/10.3791/3760>.
34. Xu K, Tian X, Oh SY, Movassaghi M, Naber SP, Kuperwasser C, et al. The fibroblast Tiam1-osteopontin pathway modulates breast cancer invasion and metastasis. *Breast Cancer Res*. 2016;18(14):14. <https://doi.org/10.1186/s13058-016-0674-8>.
35. Sawant S, Dongre H, Singh AK, Joshi S, Costea DE, Mahadik S, et al. Establishment of 3D co-culture models from different stages of human tongue tumorigenesis: utility in understanding neoplastic progression. *PLoS One*. 2016;11:e0160615. <https://doi.org/10.1371/journal.pone.0160615>.
36. Sundaram S, Johnson AR, Makowski L. Obesity, metabolism and the microenvironment: links to cancer. *J Carcinog*. 2013;12:19. <https://doi.org/10.4103/1477-3163.119606>.
37. Chkourko Gusky H, Diedrich J, MacDougald OA, Podgorski I. Omentum and bone marrow: how adipocyte-rich organs create tumour microenvironments conducive for metastatic progression. *Obes Rev*. 2016;17:1015–29. <https://doi.org/10.1111/obr.12450>.
38. Hardaway AL, Herroon MK, Rajagurubandara E, Podgorski I. Bone marrow fat: linking adipocyte-induced inflammation with skeletal metastases. *Cancer Metastasis Rev*. 2014;33:527–43. <https://doi.org/10.1007/s10555-013-9484-y>.
39. Hilvo M, Orešič M. Regulation of lipid metabolism in breast cancer provides diagnostic and therapeutic opportunities. *Clin Lipidol*. 2012;7:177–88. <https://doi.org/10.2217/clp.12.10>.
40. Nieman KM, Kenny HA, Penicka CV, Ladanyi A, Buell-Gutbrod R, Zillhardt MR, et al. Adipocytes promote ovarian cancer metastasis and provide energy for rapid tumor growth. *Nat Med*. 2011;17:1498–503. <https://doi.org/10.1038/nm.2492>.
41. Pierobon M, Frankenfeld CL. Obesity as a risk factor for triple-negative breast cancers: a systematic review and meta-analysis. *Breast Cancer Res Treat*. 2013;137:307–14. <https://doi.org/10.1007/s10549-012-2339-3>.
42. Simpson KJ, Dugan AS, Mercurio AM. Functional analysis of the contribution of RhoA and RhoC GTPases to invasive breast carcinoma. *Cancer Res*. 2004;64:8694–701. <https://doi.org/10.1158/0008-5472.CAN-04-2247>.